

**In-situ test of the
 $J(\text{BrONO}_2)/k_{\text{BrO}+\text{NO}_2}$
ratio**

S. Kreycy et al.

This discussion paper is/has been under review for the journal Atmospheric Chemistry and Physics (ACP). Please refer to the corresponding final paper in ACP if available.

Atmospheric test of the $J(\text{BrONO}_2)/k_{\text{BrO}+\text{NO}_2}$ ratio: implications for total stratospheric Br_y and bromine-mediated ozone loss

S. Kreycy¹, C. Camy-Peyret², M. P. Chipperfield³, M. Dorf¹, W. Feng⁴,
R. Hossaini³, L. Kritten⁵, B. Werner¹, and K. Pfeilsticker¹

¹Institute of Environmental Physics, University of Heidelberg, Heidelberg, Germany

²Laboratoire de Physique Moléculaire pour l'Atmosphère et l'Astrophysique (LPMAA),
Université Pierre et Marie Curie, Paris, France

³Institute for Climate and Atmospheric Science, School of Earth and Environment, University
of Leeds, Leeds, UK

⁴National Centre for Atmospheric Science, School of Earth and Environment, University of
Leeds, Leeds, UK

⁵Institute for Space Sciences, Free University Berlin, Berlin, Germany

Received: 26 September 2012 – Accepted: 8 October 2012 – Published: 23 October 2012

Correspondence to: S. Kreycy (sebastian.kreycy@iup.uni-heidelberg.de)

Published by Copernicus Publications on behalf of the European Geosciences Union.

Title Page

Abstract

Introduction

Conclusions

References

Tables

Figures

◀

▶

◀

▶

Back

Close

Full Screen / Esc

Printer-friendly Version

Interactive Discussion



Abstract

We report on time-dependent O_3 , NO_2 and BrO profile measurements taken in the stratosphere by limb observations of scattered skylight at high-latitudes during autumn circulation turn-over. The observations are complemented by simultaneous direct solar occultation measurements around sunset and sunrise performed aboard the same stratospheric balloon payload. Supporting radiative transfer and photochemical modelling indicates that, the measurements can be used to constrain the ratio $J(BrONO_2)/k_{BrO+NO_2}$, for which overall a 1.69 ± 0.04 larger ratio is found than indicated by the most recent JPL compilation (Sander et al., 2011). Sensitivity studies reveal the major reasons likely to be (1) a larger $BrONO_2$ absorption cross-section σ_{BrONO_2} , primarily for wavelengths larger than 300 nm, and (2) a smaller k_{BrO+NO_2} at 220 K than given by Sander et al. (2011). Other factors, e.g. the actinic flux and quantum yield for the dissociation of $BrONO_2$, can be ruled out.

The observations also have consequences for total inorganic stratospheric bromine (Br_y) estimated from stratospheric BrO measurements at high NO_x loadings, since the $J(BrONO_2)/k_{BrO+NO_2}$ ratio largely determines the stratospheric BrO/ Br_y ratio during daylight. Using the revised $J(BrONO_2)/k_{BrO+NO_2}$ ratio, total stratospheric Br_y is likely to be 1.4 ppt smaller than previously estimated from BrO profile measurements at high NO_x loadings. This brings estimates of total stratospheric bromine inferred from organic source gas measurements (i.e. CH_3Br , the halons, CH_2Br_2 , $CHBr_3$, ...) into closer agreement with estimates based on BrO observations (inorganic method). The consequences for stratospheric ozone due to the revised $J(BrONO_2)/k_{BrO+NO_2}$ ratio are small (maximum -0.8%), since at high NO_x (for which most Br_y assessments are made) an overestimated Br_y using the inorganic method would in return almost cancel out with the amount of reactive bromine calculated in the photochemical models.

ACPD

12, 27821–27845, 2012

In-situ test of the $J(BrONO_2)/k_{BrO+NO_2}$ ratio

S. Kreycy et al.

Title Page

Abstract

Introduction

Conclusions

References

Tables

Figures

⏪

⏩

◀

▶

Back

Close

Full Screen / Esc

Printer-friendly Version

Interactive Discussion



1 Introduction

The effect reactive bromine has on stratospheric ozone is largely dominated by the Reactions (1), (2a), and (2b) (Spencer and Rowland, 1977)



(the brackets give the recommended quantum yields Φ for $\lambda > 300$ nm), since they determine the amount of reactive bromine (BrO) and thus the bromine-mediated ozone loss in almost the whole global lower stratosphere in daytime, except in the chlorine-activated polar ozone hole regions. Sander et al. (2011) report for the termolecular Reaction (1) a 1σ uncertainty of 1.465 (at 220 K) and for the BrONO₂ absorption cross-section, $\sigma(\text{BrONO}_2)$ (Eqs. 2a and 2b) and hence for $J(\text{BrONO}_2)$ an overall uncertainty of about 1.4 (e.g. taken from Table 4.2 in JPL-2011). The former uncertainty mostly arises from the extrapolation of the laboratory measurements of $k_{\text{BrO}+\text{NO}_2}$ from high to low temperatures. The uncertainty of $\sigma(\text{BrONO}_2)$ though is due to its large decrease by 3.5 orders of magnitude with wavelength, when going from the extreme UV ($\lambda = 200$ nm) to $\lambda > 300$ nm, where the actinic fluxes, and thus the spectral contribution to $J(\text{BrONO}_2)$ strongly increases.

BrONO₂ can also be destroyed by reaction (Soller et al., 2002)



Nevertheless, Reaction (3) has a negligible effect on the lifetime of BrONO₂ below about 25 km (Sinnhuber et al., 2005), where the bulk of BrONO₂ resides during our measurements.

Title Page

Abstract

Introduction

Conclusions

References

Tables

Figures

⏪

⏩

◀

▶

Back

Close

Full Screen / Esc

Printer-friendly Version

Interactive Discussion



2 Methods

We report on spectroscopic measurements taken during a balloon flight of the LPMA/DOAS (Limb Profile Monitor of the Atmosphere/Differential Optical Absorption Spectroscopy) payload at Kiruna, Sweden (67.9° N, 22.1° E) on 7 and 8 September 2009. The payload accommodated three spectrometers: (a) a near-IR (LPMA) spectrometer that is suitable for the detection of O₃, NO₂, CH₄, N₂O, HNO₃, and other trace-gases (e.g. Camy-Peyret et al., 1995; Payan et al., 1998), (b) a UV/vis spectrometer for the high precision detection of O₃, NO₂, BrO, IO, O₄, ... in direct sunlight (e.g. Harder et al., 1998; Ferlemann et al., 2000), and (c) a UV/vis mini-DOAS instrument primarily for the detection of O₃, NO₂, and BrO in limb scattered skylight (e.g. Weidner et al., 2005; Kritten et al., 2010).

While spectrometers (a) and (b) measure in direct sun during balloon ascent, solar occultation at sunset and sunrise, the mini-DOAS instrument records the atmosphere in limb geometry, with the azimuth angle being clock-wise perpendicular ($\alpha = 90^\circ$) to the sun's azimuth direction. Viewing elevation angles are held constant ($+0.05^\circ$) during balloon ascent and but subsequently changed from $+0.6^\circ$ to -4.88° elevation angle in steps of 0.39° for the limb observations at balloon float altitude.

The balloon was launched at 14:50 UT and a solar zenith angle (SZA) of 75° on 7 September 2009 and balloon float altitude (≈ 33.5 km) was reached around 16:45 UT (SZA = 86°). The solar occultation and limb observations during sunset on 7 September 2009 lasted until 18:15 UT (SZA = 94°), and were resumed at 02:30 UT during sunrise on 8 September 2009 (SZA = 94°). They lasted until 06:00 UT (SZA = 75°), when the payload was separated from the balloon. Due to the low stratospheric winds at high-latitudes during summer/winter circulation turn-over, the balloon payload gently drifted from Kiruna to the Finish-Russian border (at around 350 km distance) within the 16-h long flight. Accordingly, due to the low shear winds the azimuth stabilisation of the balloon gondola and therefore the sun and limb pointing was extremely stable as compared to previous balloon flights (e.g. see Table 1 in Dorf et al., 2006a; Kritten et al.,

In-situ test of the J(BrONO₂)/k_{BrO+NO₂} ratio

S. Kreycky et al.

[Title Page](#)[Abstract](#)[Introduction](#)[Conclusions](#)[References](#)[Tables](#)[Figures](#)[⏪](#)[⏩](#)[◀](#)[▶](#)[Back](#)[Close](#)[Full Screen / Esc](#)[Printer-friendly Version](#)[Interactive Discussion](#)

2010). Here we primarily report on the data obtained from the spectrometers (b), and (c) obtained during sunset and of spectrometer (c) during sunrise.

For both instruments the spectral retrieval is based on the DOAS method (Platt and Stutz, 2008). Since in previous studies, they have been described at length (e.g. Weidner et al., 2005; Dorf et al., 2006a; Butz et al., 2006; Kritten et al., 2010), here only those details are described which depart from our previous work. The retrieval of O₃, NO₂, and BrO from the solar occultation and the mini-DOAS measurements is performed along the parameters as given in Butz et al. (2006) and Aliwell et al. (2002), with updates as recently described in Dorf et al. (2008), and Kritten et al. (2010). Also, the errors and uncertainties the DOAS retrievals have already been discussed in length in previous studies (e.g. Harder et al., 1998; Aliwell et al., 2002; Weidner et al., 2005; Dorf et al., 2006a; Butz et al., 2006), they are only referred to when necessary.

The limb radiances are modelled using version 2.1 of the Monte Carlo radiative transfer (RT) model McArtim (Deutschmann et al., 2011). The model's input is chosen according to measured atmospheric temperatures and pressures, including a climatological high-latitude summer aerosol profile inferred from SAGE III (http://eosweb.larc.nasa.gov/PRODOCS/sage3/table_sage3.html) and confirmed with the direct sun measurement of spectrometer (b), the balloon altitude and the geolocation, SZAs as encountered during each measurement, the azimuth and elevation angles, as well as the field of view (FOV) of the mini-DOAS telescopes. Since the mini-DOAS spectrometer is not radio-metrically calibrated, all simulations are performed relative to the first limb spectrum (elevation angle +0.6°) of each limb sequence. It is noteworthy that the radio-metric calibration does not change between the individual limb sequences, except for very high SZAs $\geq 93^\circ$, when spectrometer straylight becomes important. This finding is in agreement with the small mismatch between measured and modelled limb radiances also found by Deutschmann et al. (2011) (see Figs. 5 and 6 therein). Figure 2 indicates how well the modelled and measured relative radiances are reproduced for the limb observations at $\lambda = 350, 450, \text{ and } 495 \text{ nm}$, where BrO, NO₂ and O₃ are evaluated. The good agreement indicates that both, the relevant observation parameters (e.g. balloon

**In-situ test of the
J(BrONO₂)/k_{BrO+NO₂}
ratio**

S. Kreycky et al.

Title Page

Abstract

Introduction

Conclusions

References

Tables

Figures

◀

▶

◀

▶

Back

Close

Full Screen / Esc

Printer-friendly Version

Interactive Discussion



altitude, SZA, elevation and azimuth angles, FOV), and the atmospheric parameters (T , p , aerosol concentration, and their optical properties) are well represented in the RT model.

For the interpretation of the direct sun observations, our group's raytracing model (DAMF) is used that was extensively tested in the profile retrievals of past balloon flights (e.g. Harder et al., 2000, see Fig. 1 therein).

For the photochemical modelling the output from the most recent simulations of the 3-D CTM SLIMCAT (Chipperfield, 1999) at Kiruna for 6 September 2009 is used to initialise our lab-owned 1-D Facsimile code Labmos (e.g. Bösch et al., 2003). This approach is necessary here because the output from global SLIMCAT run is only available every 48 h. This time resolution is too coarse to be used for comparisons with measurements. On the other hand using a 1-D photochemical model for the model vs measurement inter-comparison appears justified, since during the balloon flight stratospheric winds were low, and thus very likely the same air masses were probed throughout our observations. However, both photochemical models use the most recent version of the JPL kinetics and thermochemical data for all relevant gas-phase and heterogeneous reactions (Sander et al., 2011). Finally, the Labmos simulations are constrained to the measured N_2O and CH_4 from spectrometer (a) to correct for small mismatches in the profiles of the source gases due to a small bias in the diabatic heating rate of SLIMCAT. Total stratospheric bromine (Br_y) is set to 20.3 ppt, derived from BrO observations of spectrometer (b), and the Br_y mixing ratio profile are accordingly vertically shifted (about 2 km) until the modelled and measured N_2O and CH_4 profiles matched. The initialisation is further constrained to O_3 and NO_2 obtained from the direct sun observations of spectrometer (b).

As an example of the simulations, Fig. 3 shows the simulated 2-D fields of BrO , $BrONO_2$, and $HOBr$ over Kiruna for 7 and 8 September 2009. Here, the simulation indicates that balloon soundings are well suited to study the Reactions (1), (2a), and (2b) at northern high-latitudes during the summer to winter circulation turn-over, mostly because NO_x concentrations are large and the profiles of both targeted gases (NO_2 ,

In-situ test of the $J(BrONO_2)/k_{BrO+NO_2}$ ratio

S. Kreycky et al.

Title Page

Abstract

Introduction

Conclusions

References

Tables

Figures

◀

▶

◀

▶

Back

Close

Full Screen / Esc

Printer-friendly Version

Interactive Discussion



and BrO) nicely overlap as well, thus providing a good sensitivity for Reaction (1) during sunset.

However, the Br_y partitioning at early dawn during the solar occultation measurements (the period of the red dashed lines in Fig. 3), is largely given by the efficiency of the heterogenous reaction of



at night. Therefore, our high-latitude sunrise solar occultation measurements are not considered any further here but they will be discussed in a separate study addressing the HOBr photochemistry.

In order to support an inter-comparison of measured and modelled slant column densities (SCDs) of O₃, NO₂ and BrO, the simulated photochemical fields are fed into the RT models McArtim and DAMF, where path integrals through the simulated photochemical fields are calculated and then compared with the measured SCDs.

3 Results

Figure 4 displays the inter-comparison of the measured and modelled limb SCDs of O₃, NO₂ and BrO. While for O₃ and NO₂ the agreement is close to perfect for all elevation angles and tangent heights, measured limb BrO is in general larger than obtained from the simulations for the standard run (i.e. [Br_y] = 20.3ppt, σ(BrONO₂) and k_{BrO+NO₂} from JPL-2011). This is in particular true for the high BrO SCDs values, which are obtained for large negative elevation angles (low tangent heights, or much lower altitudes than the balloon float altitude), where the bulk of BrO and BrONO₂ resides. In short, our observations indicate that during dusk BrO tends to react later (or at higher SZAs) into its major nighttime reservoir gas BrONO₂, while at dawn limb BrO tends to appear more rapidly than the standard simulation suggests.

A similar finding is obtained from the solar occultation measurements during sunset using the direct sun instrument (b) (Ferlemann et al., 2000) even though they are

less sensitive to Reactions (1), (2a), and (2b), since by definition the samples are always taken at $SZA = 90^\circ$, i.e. at the tangent height from where most of the absorption (signal) comes from (Fig. 5). Hence, our solar occultation observations mostly probe the atmosphere for a more-or-less constant $J(\text{BrONO}_2)$, but at the same time the effectively probed air masses (i.e. tangent points) move more and more away from the payload (up to 1200 km), i.e. towards the northwest during sunset. An inspection of the assimilation maps of the MIMOSA model's (http://ether.ipsl.jussieu.fr/ether/pubipsl/mimosa_2009_uk.jsp) potential vorticity (PV) indicate a negligible PV gradient at the upper level (950 K), and a small west/east PV gradient at the lower levels (475 and 550 K), indicative of different origins of both air masses. Therefore, it is likely that the kink of the measured BrO SCD at around $SZA = 92.5^\circ$ (tangent height 27 km) is not due to photochemistry, but transport. However, the measured BrO SCDs are larger than predicted by the standard model run (red line in Fig. 5). Therefore, the overall result obtained from the solar occultation measurements is similar than deduced for limb measurements, however less robust.

Both findings can be taken as evidence that, either the ratio $J(\text{BrONO}_2)/k_{\text{BrO}+\text{NO}_2}$ is larger than indicated by the JPL-2011 compilations, or that Br_y is incorrectly assumed in the model. These possibilities are investigated in the following section.

4 Discussion

In order to investigate potential causes for the deviation of the measured vs. modelled BrO SCDs, a sensitivity test for the size of the parameters $J(\text{BrONO}_2)$, $k_{\text{BrO}+\text{NO}_2}$, and Br_y is performed for limb and solar occultation measurements (Figs. 6 and 7). In both cases the best agreement between measurements and simulations is found by increasing $J(\text{BrONO}_2)$, and decreasing $k_{\text{BrO}+\text{NO}_2}$, when forcing the regression line measured vs. modelled BrO SCDs through 0. Figure 8 illustrates the situation, when varying $J(\text{BrONO}_2)$, and $k_{\text{BrO}+\text{NO}_2}$ for both, the limb (dusk and dawn) and the solar occultation measurements (dusk), whereby the colour coding denotes the slope

In-situ test of the $J(\text{BrONO}_2)/k_{\text{BrO}+\text{NO}_2}$ ratio

S. Kreycky et al.

Title Page

Abstract

Introduction

Conclusions

References

Tables

Figures

◀

▶

◀

▶

Back

Close

Full Screen / Esc

Printer-friendly Version

Interactive Discussion



In-situ test of the J(BrONO₂)/k_{BrO+NO₂} ratio

S. Kreycy et al.

Title Page

Abstract

Introduction

Conclusions

References

Tables

Figures

◀

▶

◀

▶

Back

Close

Full Screen / Esc

Printer-friendly Version

Interactive Discussion



of the regression measured vs. modelled BrO SCDs. The figure indicates that for the limb measurement the best combination of $J(\text{BrONO}_2)$, and $k_{\text{BrO}+\text{NO}_2}$ is obtained when increasing $J(\text{BrONO}_2)$ to a value of 1.1 to 1.4 and decreasing $k_{\text{BrO}+\text{NO}_2}$ to a value of 0.65 to 0.85. For the solar occultation measurements the best set of values is 0.9 to 1.4 for $J(\text{BrONO}_2)$ and 0.7 to 1 for $k_{\text{BrO}+\text{NO}_2}$. Most likely this discrepancy is due to different air masses observed by both instruments, since RT calculations show that the limb samples are taken 30–70 km right hand of the payload, but the solar occultation measurements 200–1200 km towards the sun. Merging both measurements, the best agreement is found for a ratio $J(\text{BrONO}_2)/k_{\text{BrO}+\text{NO}_2}|_{\text{obs}} = (1.69 \pm 0.04) \cdot J(\text{BrONO}_2)/k_{\text{BrO}+\text{NO}_2}|_{\text{JPL}}$, whereby less weight is put on the result of the solar occultation measurements at dusk for the reasons given above.

For this flight $[\text{Br}_y]$ was (20.3 ± 2.5) ppt (presumably in 5-yr-old air), which is determined from the direct sun measurements at balloon float using the so-called Langley method (e.g. Dorf et al., 2006b, 2008). Also note that, for the assessment of Br_y using Langley's method, stratospheric BrO is probed above balloon float, where the BrO/Br_y partitioning is mostly due to Br atoms and BrO, and thus insensitive to $J(\text{BrONO}_2)$, and/or $k_{\text{BrO}+\text{NO}_2}$.

Sensitivity runs for $[\text{Br}_y]$ within the given uncertainty range (± 2.5 ppt) are also performed (not shown). Proportionally increasing/decreasing the modelled BrO SCD by $\pm 12.5\%$ (± 2.5 ppt) slightly decreases/increases the slope of the data, but evidently not by far enough to obtain a 1 : 1 agreement between the modelled and measured BrO SCDs (Figs. 6 and 7).

Next, we address potential causes for the uncertainty in the $J(\text{BrONO}_2)/k_{\text{BrO}+\text{NO}_2}$ ratio. Incorrect modelled actinic fluxes by the required amount are rather unlikely, since our RT model nicely explains the measured limb radiances at different wavelengths, different elevation angles and SZAs (e.g. see Fig. 2, Bösch et al., 2001, and Fig. 5 in Deutschmann et al., 2011). Also the largely dominant contribution of the direct solar irradiance to the actinic flux seems to be well understood (e.g. Bösch et al., 2001; Gurlit et al., 2005). Moreover, since our measurement is insensitive to the quantum yields (Φ)

of Reactions (2a) and (2b) (the Br atoms formed in Reaction (2b) would readily react with O_3 to form BrO), an incorrect $J(\text{BrONO}_2)$ points to an incorrect $\sigma(\text{BrONO}_2)$. For $J(\text{BrONO}_2)$ JPL-2011 states an overall uncertainty of 1.4 (Table 4.2) most likely due to uncertainties of $\sigma(\text{BrONO}_2)$ in the UV-A and visible, and its temperature dependence.

5 Since at $T = 298 \text{ K}$ $\sigma(\text{BrONO}_2)$ agrees fairly well among the different studies, one may speculate whether the recommended temperature correction for $T = 220 \text{ K}$ is in fact too strong. Furthermore, JPL-2011 states a 1σ uncertainty of 1.465 for $k_{\text{BrO}+\text{NO}_2}$ at 220 K. Here, the major uncertainty arises from the T-dependence of the high pressure limit of the reaction, which is found to be rather large ($m = 2.9$). Attempts to fit the data with the JPL master equation analysis was found to be insufficient to fit the data at low pressures (Sander et al., 2011). Therefore, one may again speculate as to whether $k_{\text{BrO}+\text{NO}_2}$ at 220 K is somewhat lower than recommended by JPL-2011.

10 The finding has also implications for total stratospheric bromine. Using the inorganic method to assess stratospheric Br_y relies on a photochemical correction, i.e. Br_y is calculated from measured BrO according to $[\text{BrO}] = [\text{Br}_y] \cdot (1 + k_{\text{BrO}+\text{NO}_2} \cdot [\text{NO}_2] \cdot [\text{M}] / J_{\text{BrONO}_2} \dots)$ where “...” indicates contributions from minor bromine species in the stratosphere (e.g. HOBr, Br, BrCl, and HBr). In our case, taking the revised $J(\text{BrONO}_2)/k_{\text{BrO}+\text{NO}_2}$ ratio (i.e. 1.69 ± 0.04), stratospheric Br_y may decrease by as much as 1.4 ppt. In fact, a smaller Br_y assessed using the inorganic method would tend to close the existing gap to total stratospheric bromine assessed using measurements of organic source gases. Also the potential contribution of so-called very short-lived substances (VSLS) to stratospheric bromine would accordingly decrease. For example, while our assessment of Br_y for 4.5 old air probed over Brazil in 2005 indicated a VSLS contribution of $[\text{VSLS}]_{\text{inorg}} = (5.2 \pm 2.5) \text{ ppt}$ (Dorf et al., 2008), the organic method resulted in only $[\text{VSLS}]_{\text{org}} = (1.25 \pm 0.08) \text{ ppt}$ (Laube et al., 2008). A more recent comparison indicated $[\text{VSLS}]_{\text{inorg}} = (3.5 \pm 2.5) \text{ ppt}$ (inferred from our own BrO measurement using the Langley method) and about $[\text{VSLS}]_{\text{org}} = 2.25 \text{ ppt}$ (Brinckmann et al., 2012), for the air masses jointly probed by both methods over Brazil in 2008.

In-situ test of the $J(\text{BrONO}_2)/k_{\text{BrO}+\text{NO}_2}$ ratio

S. Kreycky et al.

[Title Page](#)[Abstract](#)[Introduction](#)[Conclusions](#)[References](#)[Tables](#)[Figures](#)[◀](#)[▶](#)[◀](#)[▶](#)[Back](#)[Close](#)[Full Screen / Esc](#)[Printer-friendly Version](#)[Interactive Discussion](#)

**In-situ test of the
J(BrONO₂)/k_{BrO+NO₂}
ratio**

S. Kreycy et al.

Title Page

Abstract

Introduction

Conclusions

References

Tables

Figures

◀

▶

◀

▶

Back

Close

Full Screen / Esc

Printer-friendly Version

Interactive Discussion



The implications of our finding for stratospheric ozone loss are small or even negligible, since the ozone loss by the BrONO₂ photolysis has a small contribution to the total ozone loss by bromine (dominated by the reaction BrO + ClO), which is presently assessed to amount to about 30–35 % on a global average (Sinnhuber et al., 2009).

Furthermore, even though BrONO₂ mostly photolyses into Br + NO₃ (Reaction 2b), only about 12 % of the produced NO₃ photolyses into the channel NO + O₂, which in fact may cause some ozone loss (via reformation of BrO and NO₂ and the consumption of two ozone molecules). A possibly larger impact would be through the altered partitioning of bromine between BrO and its reservoir BrONO₂, as BrO participates in a number of ozone loss cycles.

To quantify the impact of our findings two runs with the SLIMCAT off-line 3-D CTM are performed (e.g. Chipperfield, 2006; Feng et al., 2007). The runs are initialised in November 2008 from an existing SLIMCAT run and integrated for 14 months using ECMWF meteorology. The model run has a horizontal resolution of 2.8° × 2.8° and included a detailed stratospheric chemistry scheme (Chipperfield, 1999). One model run is performed with standard JPL kinetics. In the other run J(BrONO₂) is scaled by 1.27 and k_{BrO+NO₂} was scaled by 0.75, thereby scaling the ratio J(BrONO₂)/k_{BrO+NO₂} by 1.69. Figure 9 shows the percentage ozone difference between these runs for 2009 as an annual mean zonal mean and as a zonal mean at 18 km altitude. Overall the impact of these kinetic changes on stratospheric ozone is small and confined to altitudes below about 30 km where BrONO₂ is a reservoir for bromine. The largest decrease in ozone is around 0.8 % at the edge of the Antarctic ozone region in September/October. The kinetics changes lead to less BrONO₂ (and HOBr) and more bromine in the form of BrO which catalyses ozone loss. The small effect itself is more important at the edge of the polar vortex and late in the season when NO_y is more readily available to form BrONO₂. Smaller changes are seen in the Arctic and at mid-latitudes.

In consequence, an increase in the photolysis rate and a decrease in the formation rate of BrONO₂ as determined here would eventually imply only a small change in the bromine-mediated ozone loss in the stratosphere.

5 Conclusions

We performed an atmospheric test of the $J(\text{BrONO}_2)/k_{\text{BrO}+\text{NO}_2}$ ratio assisted by photochemical and radiative transfer modelling. It is found that under stratospheric conditions ($T \approx 220 \text{ K}$ and $p = 50 \text{ mbar}$), the ratio $J(\text{BrONO}_2)/k_{\text{BrO}+\text{NO}_2}$ is 1.69 ± 0.04 larger than given in the JPL-2011 compilation. Our sensitivity study indicates that very likely both $\sigma(\text{BrONO}_2)$ and $k_{\text{BrO}+\text{NO}_2}$ differ from the JPL-2011 recommendation.

The major consequences of our study are threefold. (1) Recent assessments of total stratospheric bromine using the inorganic method during high stratospheric NO_x loadings may have overestimated the necessary correction for the BrO to Br_y ratio. As a consequence, stratospheric $[\text{Br}_y]$ should be 1.4 ppt lower, which amounts to 6.8 % of the total stratospheric bromine. (2) A larger $J(\text{BrONO}_2)/k_{\text{BrO}+\text{NO}_2}$ ratio may also cause a small increase (maximum -0.8%) in the bromine-mediated ozone loss in the stratosphere, because ozone loss by BrONO_2 , and its products is anyhow small. Also an overestimated stratospheric Br_y due to an incorrect $J(\text{BrONO}_2)/k_{\text{BrO}+\text{NO}_2}$ ratio would be compensated in the photochemical models, when reactive bromine is calculated using the inorganic method. (3) In the troposphere, a diminished formation of BrONO_2 where high NO_x meets reactive bromine released from the degradation of organic bromine compounds, or bromine being heterogeneously released from salty aerosols or salt lakes, may lead to a longer lifetime of ozone destroying BrO. In consequence, the revised $J(\text{BrONO}_2)/k_{\text{BrO}+\text{NO}_2}$ ratio may cause more ozone destruction and a more efficient degradation of organic molecules by their reaction with Br atoms on one hand. On the other hand it may hinder the activation of reactive bromine tied to the aerosol or in bulk salt (e.g. von Glasow et al., 2004; Salawitch, 2006). Accordingly, the consequences of our finding for ozone, and the oxidation capacity, in the troposphere may largely depend on the specific conditions.

Acknowledgements. This study was funded by through the grants of the German ministry of Economy (BMWi) (50EE0840), the European Space Agency (ESA-ESRIN: no. RFQ/3-12092/07/I-OL) and the Deutsche Forschungsgemeinschaft, DFG (grants PF-384/5-1 and

In-situ test of the $J(\text{BrONO}_2)/k_{\text{BrO}+\text{NO}_2}$ ratio

S. Kreycy et al.

Title Page

Abstract

Introduction

Conclusions

References

Tables

Figures

◀

▶

◀

▶

Back

Close

Full Screen / Esc

Printer-friendly Version

Interactive Discussion



384/5-1 and PF384/9-1/2). Additional funding from the EU projects Reconcile (FP7-ENV-2008-1-226365), and SHIVA (FP7-ENV-2007-1-226224) is highly acknowledged. The SLIMCAT modelling was supported by the NERC National Centre for Atmospheric Science (NCAS), UK. We thank the CNES equipe nacelles pointées and the balloon team from Aire sur l'Adour/France without which the balloon flight would not have been possible. We also thank our colleagues from the LPMA balloon team (P. Jeseck, I. Pepin and Y. Té) for the successful cooperation. Finally we are grateful for the hospitality and support given by the personnel of Esrange/Kiruna to successfully perform the balloon flight.

References

- Aliwell, S., Van Roozendaal, M., Johnston, P., Richter, A., Wagner, T., Arlander, D., Burrows, J., Fish, D., Jones, R., Tornkvist, K., Lambert, J.-C., Pfeilsticker, K., and Pundt, I.: Analysis for BrO in zenith-sky spectra: an intercomparison exercise for analysis improvement, *J. Geophys. Res.*, 107, 4199, doi:10.1029/2001JD000329, 2002. 27825
- Bösch, H., Camy-Peyret, C., Chipperfield, M. P., Fitzenberger, R., Harder, H., Schiller, C., Schneider, M., Trautmann, T., and Pfeilsticker, K.: Comparison of measured and modeled stratospheric UV/visible actinic fluxes at large solar zenith angles, *Geophys. Res. Lett.*, 28, 1179–1182, 2001. 27829
- Bösch, H., Camy-Peyret, C., Chipperfield, M. P., Fitzenberger, R., Harder, H., Platt, U., and Pfeilsticker, K.: Upper limits of stratospheric IO and OIO inferred from center-to-limb-darkening-corrected balloon-borne solar occultation visible spectra: implications for total gaseous iodine and stratospheric ozone, *J. Geophys. Res.*, 108, 4455, doi:10.1029/2002JD003078, 2003. 27826
- Brinckmann, S., Engel, A., Bönisch, H., Quack, B., and Atlas, E.: Short-lived brominated hydrocarbons – observations in the source regions and the tropical tropopause layer, *Atmos. Chem. Phys.*, 12, 1213–1228, doi:10.5194/acp-12-1213-2012, 2012. 27830
- Butz, A., Bösch, H., Camy-Peyret, C., Chipperfield, M., Dorf, M., Dufour, G., Grunow, K., Jeseck, P., Kühl, S., Payan, S., Pepin, I., Pukite, J., Rozanov, A., von Savigny, C., Sioris, C., Wagner, T., Weidner, F., and Pfeilsticker, K.: Inter-comparison of stratospheric O₃ and NO₂ abundances retrieved from balloon borne direct sun observations and Envisat/SCIAMACHY

In-situ test of the J(BrONO₂)/k_{BrO}+NO₂ ratio

S. Kreycky et al.

Title Page

Abstract

Introduction

Conclusions

References

Tables

Figures

◀

▶

◀

▶

Back

Close

Full Screen / Esc

Printer-friendly Version

Interactive Discussion



**In-situ test of the
 $J(\text{BrONO}_2)/k_{\text{BrO}+\text{NO}_2}$
ratio**

S. Kreycy et al.

Title Page

Abstract

Introduction

Conclusions

References

Tables

Figures

◀

▶

◀

▶

Back

Close

Full Screen / Esc

Printer-friendly Version

Interactive Discussion



limb measurements, *Atmos. Chem. Phys.*, 6, 1293–1314, doi:10.5194/acp-6-1293-2006, 2006. 27825

Camy-Peyret, C., Jeseck, P., Payan, S., Hawat, T., Durry, G., and Flaud, J.-M.: Comparison of CH_4 and N_2O profiles at high and mid-latitudes using the LPMA balloon borne Fourier Transform instrument, in: *Air Pollution Research Report, Polar Stratospheric Ozone Symposium*, Schliersee, 1995. 27824

Chipperfield, M. P.: Multiannual simulations with a three-dimensional chemical transport model, *J. Geophys. Res.*, 104, 1781–1805, 1999. 27826, 27831

Chipperfield, M. P.: New version of the TOMCAT/SLIMCAT off-line chemical transport model: intercomparison of stratospheric tracer experiments, *Q. J. Roy. Meteorol. Soc.*, 132, 1179–1203, 2006. 27831

Deutschmann, T., Beirle, S., Frieß, U., Grzegorski, M., Kern, C., Kritten, L., Platt, U., Puķite, J., Wagner, T., Werner, B., and Pfeilsticker, K.: The Monte Carlo atmospheric radiative transfer model McArtim: introduction and validation of Jacobians and 3D features, *J. Quant. Spectrosc. Ra.*, 112, 1119–1137, 2011. 27825, 27829

Dorf, M., Bösch, H., Butz, A., Camy-Peyret, C., Chipperfield, M. P., Engel, A., Goutail, F., Grunow, K., Hendrick, F., Hrechanyy, S., Naujokat, B., Pommereau, J. P., Van Roozendaal, M., Sioris, C., Stroh, F., Weidner, F., and Pfeilsticker, K.: Balloon-borne stratospheric BrO measurements: comparison with Envisat/SCIAMACHY BrO limb profiles, *Atmos. Chem. Phys.*, 6, 2483–2501, doi:10.5194/acp-6-2483-2006, 2006a. 27824, 27825

Dorf, M., Butler, J., Butz, A., Camy-Peyret, C., Chipperfield, M., Kritten, L., Montzka, S., Simmes, B., Weidner, F., and Pfeilsticker, K.: Long-term observations of stratospheric bromine reveal slow down in growth, *Geophys. Res. Lett.*, 33, L24803, doi:10.1029/2006GL027714, 2006b. 27829

Dorf, M., Butz, A., Camy-Peyret, C., Chipperfield, M. P., Kritten, L., and Pfeilsticker, K.: Bromine in the tropical troposphere and stratosphere as derived from balloon-borne BrO observations, *Atmos. Chem. Phys.*, 8, 7265–7271, doi:10.5194/acp-8-7265-2008, 2008. 27825, 27829, 27830

Feng, W., Chipperfield, M., Davies, S., von der Gathen, S., Kyro, E., Volk, C., Ulanovsky, A., and Belyaev, G.: Large chemical ozone loss in 2004/05 Arctic Winter/Spring, *Geophys. Res. Lett.*, 34, L09803, doi:10.1029/2006GL029098, 2007. 27831

Ferlemann, F., Bauer, N., Fitzenberger, R., Harder, H., Osterkamp, H., Perner, D., Platt, U., Scheider, M., Vradelis, P., and Pfeilsticker, K.: Differential optical absorption spectroscopy

instrument for stratospheric balloon-borne trace gas studies, Appl. Opt., 39, 2377–2386, 2000. 27824, 27827

Gurlit, W., Bösch, H., Bovensmann, H., Burrows, J. P., Butz, A., Camy-Peyret, C., Dorf, M., Gerilowski, K., Lindner, A., Noël, S., Platt, U., Weidner, F., and Pfeilsticker, K.: The UV-A and visible solar irradiance spectrum: inter-comparison of absolutely calibrated, spectrally medium resolution solar irradiance spectra from balloon- and satellite-borne measurements, Atmos. Chem. Phys., 5, 1879–1890, doi:10.5194/acp-5-1879-2005, 2005. 27829

Harder, H., Camy-Peyret, C., Ferlemann, F., Fitzenberger, R., Hawat, T., Osterkamp, H., Schneider, M., Perner, D., Platt, U., Vradelis, P., and Pfeilsticker, K.: Stratospheric BrO profiles measured at different latitudes and seasons: atmospheric observations, Geophys. Res. Lett., 25, 3843–3846, 1998. 27824, 27825

Harder, H., Bösch, H., Camy-Peyret, C., Chipperfield, M., Fitzenberger, R., Payan, S., Perner, D., Platt, U., Sinnhuber, B.-M., and Pfeilsticker, K.: Comparison of measured and modeled Stratospheric BrO: implications for the total amount of stratospheric bromine, Geophys. Res. Lett., 27, 3695–3698, 2000. 27826

Kritten, L., Butz, A., Dorf, M., Deutschmann, T., Köhl, S., Prados-Roman, C., Puķīte, J., Rozanov, A., Schofield, R., and Pfeilsticker, K.: Time dependent profile retrieval of UV/vis absorbing radicals from balloon-borne limb measurements – a case study on NO₂ and O₃, Atmos. Meas. Tech., 3, 933–946, doi:10.5194/amt-3-933-2010, 2010. 27824, 27825

Laube, J. C., Engel, A., Bönisch, H., Möbius, T., Worton, D. R., Sturges, W. T., Grunow, K., and Schmidt, U.: Contribution of very short-lived organic substances to stratospheric chlorine and bromine in the tropics – a case study, Atmos. Chem. Phys., 8, 7325–7334, doi:10.5194/acp-8-7325-2008, 2008. 27830

Payan, S., Camy-Peyret, C., Jeseck, P., Hawat, T., Durry, G., and Lefèvre, F.: First direct simultaneous HCl and ClONO₂ profile measurements in the arctic vortex, Geophys. Res. Lett., 25, 2663–2666, 1998. 27824

Platt, U. and Stutz, J.: Differential Optical Absorption Spectroscopy (DOAS), Principle and Applications, ISBN 3-340-21193-4, Springer Verlag, Heidelberg, 2008. 27825

Salawitch, R.: Atmospheric chemistry: biogenic bromine, Nature, 439, 275–277, 2006. 27832

Sander, S., Friedl, R. R., Barkern, J., Golden, D., Kurylo, M., Wine, P., Abbat, J., Burkholder, J., Moortgaret, C., Huie, R., and Orkin, R. E.: Chemical kinetics and photochemical data for use in atmospheric studies, Technical Report, NASA/JPL Publication, 17, 2011. 27822, 27823, 27826, 27830

ACPD

12, 27821–27845, 2012

In-situ test of the J(BrONO₂)/k_{BrO+NO₂} ratio

S. Kreycky et al.

Title Page

Abstract

Introduction

Conclusions

References

Tables

Figures

◀

▶

◀

▶

Back

Close

Full Screen / Esc

Printer-friendly Version

Interactive Discussion



**In-situ test of the
 $J(\text{BrONO}_2)/k_{\text{BrO}+\text{NO}_2}$
ratio**S. Kreycy et al.

[Title Page](#)[Abstract](#)[Introduction](#)[Conclusions](#)[References](#)[Tables](#)[Figures](#)[⏪](#)[⏩](#)[◀](#)[▶](#)[Back](#)[Close](#)[Full Screen / Esc](#)[Printer-friendly Version](#)[Interactive Discussion](#)

- Sinnhuber, B.-M., Rozanov, A., Sheode, N., Afe, O. T., Richter, A., Sinnhuber, M., Wittrock, F., Burrows, J. P., Stiller, G. P., von Clarmann, T., and Linden, A.: Global observations of stratospheric bromine monoxide from SCIAMACHY, *Geophys. Res. Lett.*, 32, 1–5, 2005. 27823
- 5 Sinnhuber, B.-M., Sheode, N., Sinnhuber, M., Chipperfield, M. P., and Feng, W.: The contribution of anthropogenic bromine emissions to past stratospheric ozone trends: a modelling study, *Atmos. Chem. Phys.*, 9, 2863–2871, doi:10.5194/acp-9-2863-2009, 2009. 27831
- Soller, R., Nicovich, J., and Wine, P.: Bromine nitrate photochemistry: quantum yields for O, Br, and BrO over the wavelength range 248–355 nm, *J. Phys. Chem. A*, 106, 8378–8385, 2002. 27823
- 10 Spencer, J. E. and Rowland, F. S.: Bromine nitrate and its stratospheric significance, *J. Phys. Chem.*, 82, 7–10, 1977. 27823
- von Glasow, R., von Kuhlmann, R., Lawrence, M. G., Platt, U., and Crutzen, P. J.: Impact of reactive bromine chemistry in the troposphere, *Atmos. Chem. Phys.*, 4, 2481–2497, doi:10.5194/acp-4-2481-2004, 2004. 27832
- 15 Weidner, F., Bösch, H., Bovensmann, H., Burrows, J. P., Butz, A., Camy-Peyret, C., Dorf, M., Gerilowski, K., Gurlit, W., Platt, U., von Friedeburg, C., Wagner, T., and Pfeilsticker, K.: Balloon-borne limb profiling of UV/vis skylight radiances, O₃, NO₂, and BrO: technical set-up and validation of the method, *Atmos. Chem. Phys.*, 5, 1409–1422, doi:10.5194/acp-5-1409-2005, 2005. 27824, 27825

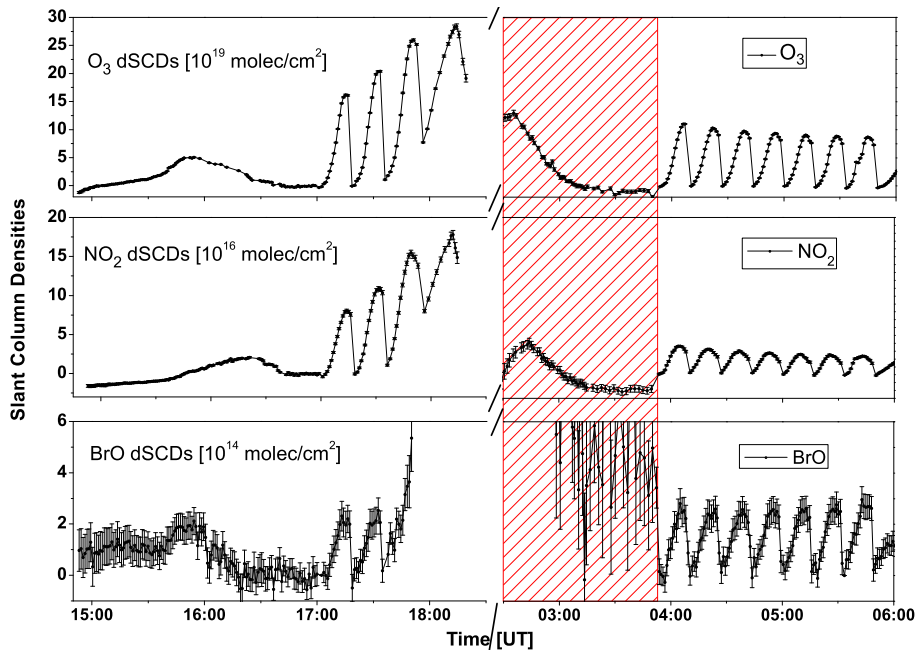


Fig. 1. Measured slant column densities of O_3 (upper panel), NO_2 (middle panel), and BrO (lower panel) in limb geometry during the balloon flight from Kiruna on 7 and 8 September 2009. During balloon ascent from 14:50 UT until 17:10 UT, the limb radiation was observed for an elevation angle of 0.05° . During dusk (17:10 UT to 18:30 UT), 3.5 limb scans were performed at 33 km altitude. During early dawn, the scanning telescope malfunctioned (the reddish area), and the limb scans (in total 7.25) started at 03:55 UT and commenced until 06:00 UT, when the balloon was floating at 31 km altitude. Each limb scan consists of limb observations at $+0.6^\circ$, in steps of 0.39° down -4.88° elevation angle.

In-situ test of the $J(BrONO_2)/k_{BrO+NO_2}$ ratio

S. Kreycy et al.

Title Page

Abstract

Introduction

Conclusions

References

Tables

Figures

◀

▶

◀

▶

Back

Close

Full Screen / Esc

Printer-friendly Version

Interactive Discussion



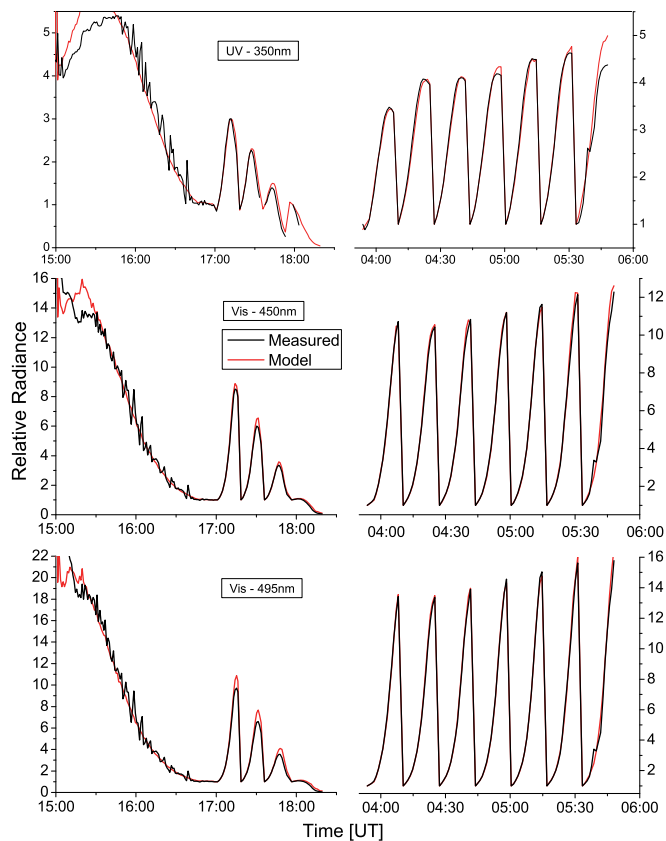


Fig. 2. Inter-comparison of measured (black) and modelled (red) relative radiances at $\lambda = 350$, 450, and 495 nm for the limb scans as described in the legend of Fig. 1. The RT simulations are normalised for the balloon ascent to the observations at 17:00 UT, and for each limb scan to the observation for the largest elevation angle (0.6°), i.e. for the lowest radiiances.

In-situ test of the $J(\text{BrONO}_2)/k_{\text{BrO}+\text{NO}_2}$ ratio

S. Kreycy et al.

Title Page

Abstract Introduction

Conclusions References

Tables Figures

◀ ▶

◀ ▶

Back Close

Full Screen / Esc

Printer-friendly Version

Interactive Discussion



In-situ test of the $J(\text{BrONO}_2)/k_{\text{BrO}+\text{NO}_2}$ ratio

S. Kreycy et al.

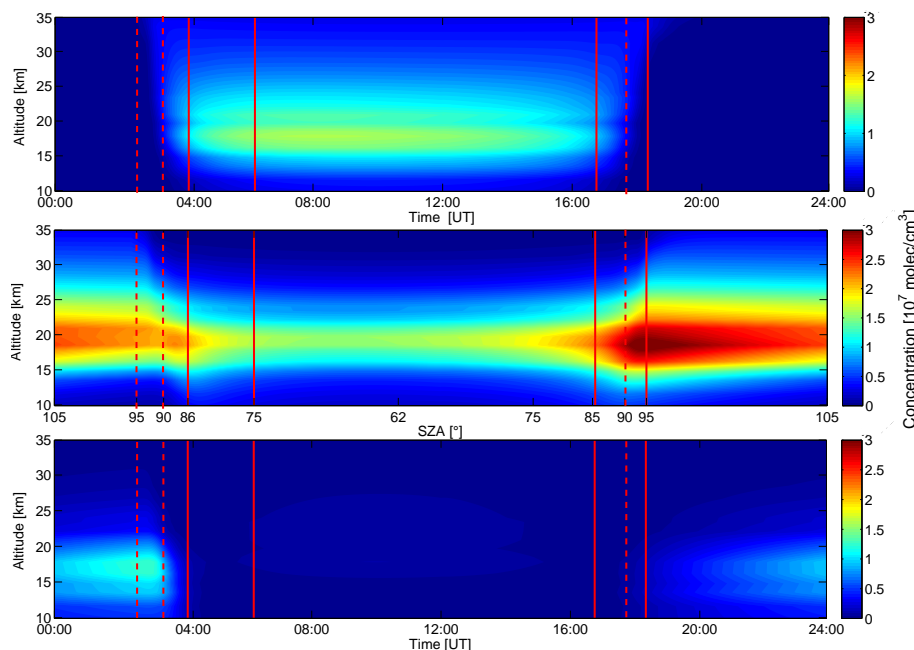


Fig. 3. Standard simulation of the key stratospheric bromine species for 7 September 2009 using the Labmos photochemical model: diurnal variation of BrO (upper panel), BrONO₂ (middle panel), and HOBr (lower panel). The red drawn lines indicate the periods of the limb measurements (local SZA = 86–75° at a.m. and 85–95° at p.m.) and the dashed red lines the period of the direct sunlight measurements (local SZA = 95–90° at a.m., and SZA = 90–95° at p.m.). Solar zenith angles shown in the middle panel refer to local angles and the colour coding indicates the respective concentrations in units of $10^7 \text{ molec cm}^{-3}$.

Title Page

Abstract

Introduction

Conclusions

References

Tables

Figures

◀

▶

◀

▶

Back

Close

Full Screen / Esc

Printer-friendly Version

Interactive Discussion



**In-situ test of the
 $J(\text{BrONO}_2)/k_{\text{BrO}+\text{NO}_2}$
ratio**

S. Kreycy et al.

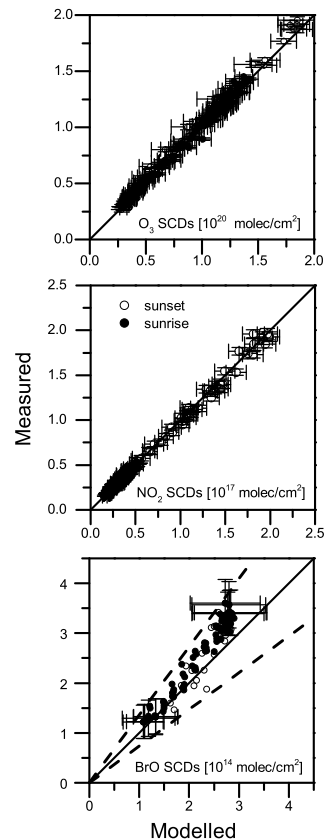


Fig. 4. Inter-comparison of limb measured vs. modelled slant column concentrations of O_3 (upper panel), NO_2 (middle panel) and BrO (lower panel) for the standard JPL-2011 kinetics in units of given in the panels. Note the excellent agreement for the slant column densities O_3 and NO_2 , but the fair agreement for BrO with standard model parameters. In the lower panel the JPL-2011 uncertainty of the $J(\text{BrONO}_2)/k_{\text{BrO}+\text{NO}_2}$ ratio is indicated (dashed lines).

Title Page

Abstract

Introduction

Conclusions

References

Tables

Figures

◀

▶

◀

▶

Back

Close

Full Screen / Esc

Printer-friendly Version

Interactive Discussion



In-situ test of the $J(\text{BrONO}_2)/k_{\text{BrO}+\text{NO}_2}$ ratio

S. Kreycy et al.

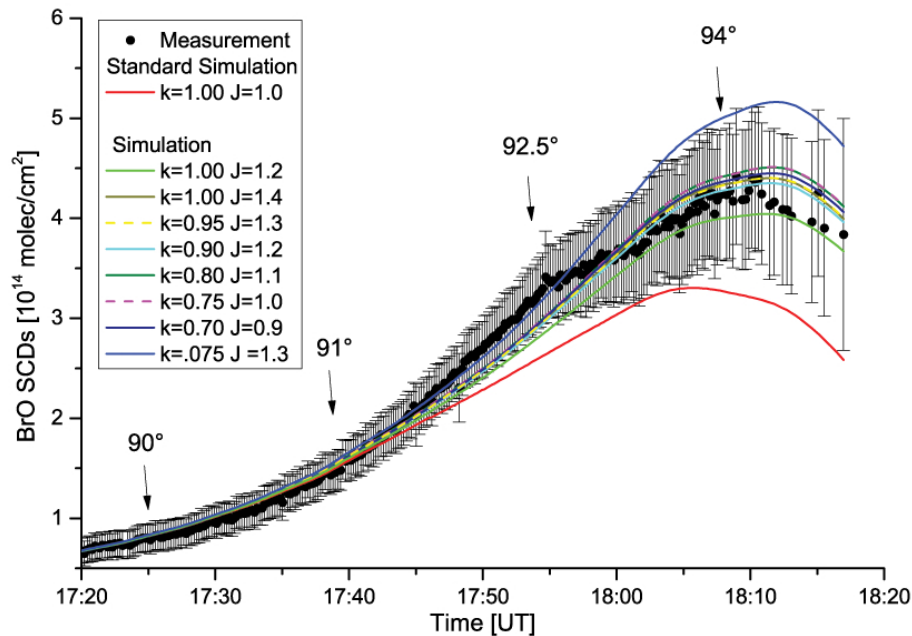


Fig. 5. Inter-comparison of measured vs. modelled slant column densities of BrO for the sunset solar occultation measurements on 7 September 2009. The coloured lines show simulations for different pairs of $J(\text{BrONO}_2)$ and $k_{\text{BrO}+\text{NO}_2}$ as indicated by the insert. Local solar zenith angles (e.g. 90°, 91°, 92.5°, and 94°) of some measurements are also indicated.

In-situ test of the $J(\text{BrONO}_2)/k_{\text{BrO}+\text{NO}_2}$ ratio

S. Kreycy et al.

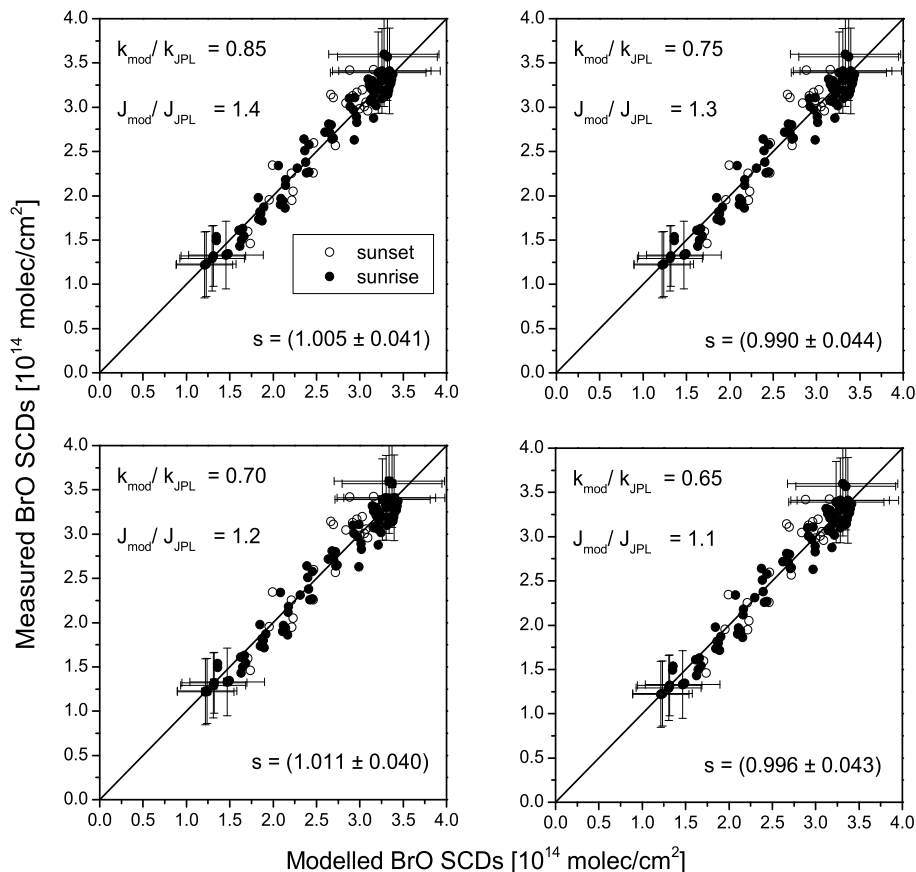


Fig. 6. Inter-comparison of limb measured vs. modelled slant column densities of BrO for different scaling factors of $J(\text{BrONO}_2)$ and $k_{\text{BrO}+\text{NO}_2}$ as indicated in the individual panels. The open dots are for sunset and the full dots for sunrise observations. The s-value indicates the slope and its uncertainty between modelled and measured BrO SCDs.

Title Page

Abstract

Introduction

Conclusions

References

Tables

Figures

◀

▶

◀

▶

Back

Close

Full Screen / Esc

Printer-friendly Version

Interactive Discussion

In-situ test of the $J(\text{BrONO}_2)/k_{\text{BrO}+\text{NO}_2}$ ratio

S. Kreycky et al.

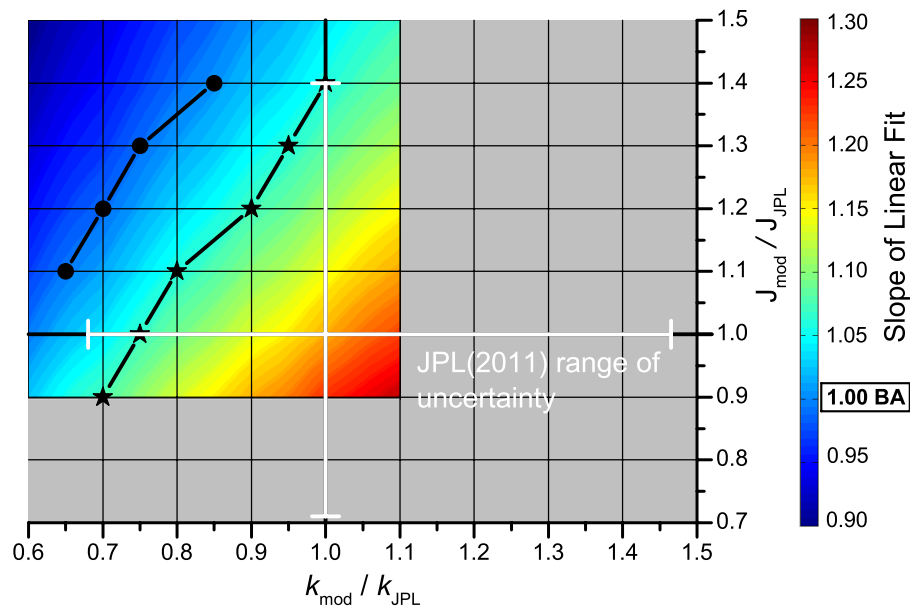


Fig. 8. Regression of $J(\text{BrONO}_2)$ vs. $k_{\text{BrO}+\text{NO}_2}$ for the limb (black dots) and solar occultation BrO measurements (black stars) together with the uncertainty range for both parameters as indicated by the JPL-2011 compilation. The colour coding indicates the resulting slopes of the modelled vs. measured BrO SCD regression, when forcing the regression line through zero. So the best agreement (BA) is given for a slope of 1.

Title Page

Abstract Introduction

Conclusions References

Tables Figures

◀ ▶

◀ ▶

Back Close

Full Screen / Esc

Printer-friendly Version

Interactive Discussion



In-situ test of the $J(\text{BrONO}_2)/k_{\text{BrO}+\text{NO}_2}$ ratio

S. Kreycy et al.

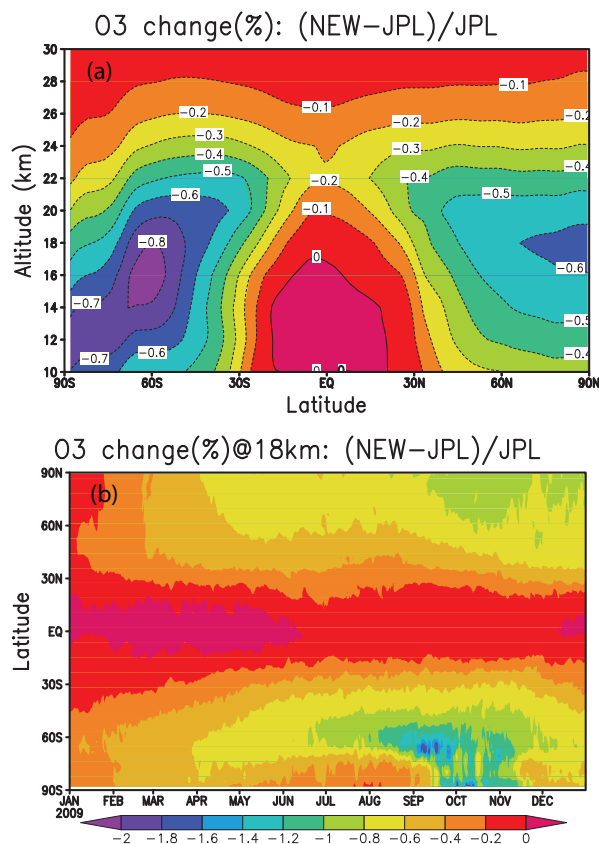


Fig. 9. Difference in ozone from a simulation of the SLIMCAT 3-D CTM with scaled $J(\text{BrONO}_2)$ ($\times 1.27$) and $k_{\text{BrO}+\text{NO}_2}$ ($\times 0.75$) compared to a run with standard JPL kinetics. **(a)** Difference (%) in zonal mean annual mean ozone and **(b)** difference (%) in zonal mean ozone at 18 km as a function of time. Note the different colour scales in the two panels.

Title Page

Abstract Introduction

Conclusions References

Tables Figures

◀ ▶

◀ ▶

Back Close

Full Screen / Esc

Printer-friendly Version

Interactive Discussion

